Lignin-Based Activated Carbon Fibers and Controllable Pore Size and Properties

Qing Shen, Tao Zhang, Wen-Xin Zhang, Shuai Chen, Mebrahtu Mezgebe

State Key Laboratory for Modification of Chemical Fiber and Polymer Materials, Polymer Department of Donghua University, 201620 Songjiang, Shanghai, China

Received 8 July 2010; accepted 31 October 2010
DOI 10.1002/app.33701
Published online 25 February 2011 in Wiley Online Library (wileyonlinelibrary.com).

ABSTRACT: Several lignin-based activated carbon fibers (ACFs) were prepared by initial synthesis of lignin–phenol–formaldehyde (LPF) resins with varied lignin contents, 8–20%, respectively, and then the melt spinning and thermal treatments. Because the guaiacyl groups of lignin reacted with the formaldehyde, the role of lignin played becomes a dominator for controlling the thermal properties of LPF resin and the pore size and related properties of ACFs. This was proven by the comparison of the scanning electron microscope photographs of all prepared ACFs. FTIR spectra showed that the ACFs were structured by lignin-contributed carbons. The porosity and adsorption behavior of these ACFs were also studied and compared. Results showed that the ACFs with 14% lignin content have better pore structure and adsorption properties. © 2011 Wiley Periodicals, Inc. J Appl Polym Sci 121: 989–994, 2011

Key words: lignin; activated carbon fiber; pore size; properties; controllable

INTRODUCTION

As one kind of carbon materials, the activated carbon fibers (ACFs) have been broadly studied and applied.[1,2] Noted to control, the pore structure is necessary and required for the fabrication of ACFs.[3–11]

Considering that the phenolic resin has been broadly applied to prepare ACFs,[4,5] and the lignin is one of the most abundant biomacromolecules existing in the plant kingdom, which has the phenyl–propane structure similar to the phenol–formaldehyde resin,[12,13] recently, we therefore took lignin to replace the phenol/formaldehyde to prepare a phenolic resin and then furthermore to apply this resin to fabricate lignin-based carbon films.[14]

Because the lignin was found a dominator of the carbon film structure,[14] it is furthermore aimed to apply lignin to fabricate ACFs with controllable structure and properties.

EXPERIMENTAL

Materials

As previously described,[14] the powder alkali lignin purchased from Tokyo Chemical Industry Co., Japan, was used as received. According to the suppler, this lignin has the molecular weight M_w of about 28,000 and M_n 5000.

The phenol (99.5%), formaldehyde (37%), and sodium hydroxide (97%) all in analytic grade were purchased from local chemical company at Shanghai and used without further purification.

Synthesis of lignin–phenol–formaldehyde and preparation of activated carbon fiber

The synthesis of lignin–phenol–formaldehyde (LPF) resin was initially carried out in the presence of 0.1*M* NaOH as the same as previously.[14] To mix the phenol and formaldehyde with a molar ratio of 6 : 7, this hybrid was charged into a reactor, and a NaOH solution was then added to keep the mixture under an alkaline condition to start the reaction. The lignin powder was subsequently added with different contents, for example, 8, 14, and 20 wt %, respectively. The mixture was then heated to about 95°C and kept until the resol resin was formed.[15,16] After cooling, the LPF resin fibers were spun via wet spinning using HCl/formaldehyde (1 : 1) solution as coagulator.[17] The thermal treatment was performed as two steps, the first is to oxide the as-spun fibers (ASFs) in air atmosphere by heating the temperature from 25 to 250°C at a rate of 2°C/min and kept for 1 h. The second is performed under nitrogen atmosphere by heating the temperature from 250 to 800°C at a rate of 180°C/h and kept for another 1 h.

Correspondence to: Q. Shen (sqing@dhu.edu.cn).
Contract grant sponsor: Programmers of Introducing Talents of Discipline to Chinese Universities; contract grant number: 111-2-04.

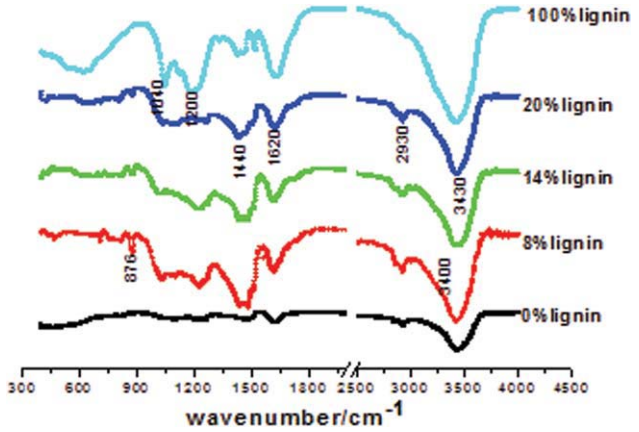

Figure 1 FTIR spectra of lignin, LPF resin, and neat resin. [Color figure can be viewed in the online issue, which is available at wileyonlinelibrary.com.]

Analysis and characterization

The FTIR spectra of all samples were recorded from 400 to 4000 cm^{-1} using a Nicolet NEXUS-670 FTIR spectrometer after scanning of 10 times in a resolution of 4 cm^{-1}.

Thermogravimetric analysis (TGA) was performed using a TGA/DTA TG209F1 Netzsch instrument under nitrogen atmosphere. During this process, a constant heating rate, for example, of 10°C/min was applied to heat the temperature of samples from 30 to 800°C.

The elemental analysis (EA) was performed using a Vario EL III element analyzer. The samples, for example, the ASFs, preoxidized fibers (POFs), and ACFs, all with 20% lignin content were analyzed of their C, H, N, and O element contents, respectively.

The pore sizes of ACFs were estimated by scanning electron microscope (SEM; *S*-3000N) with an accelerating voltage of about 15 kV and magnification of 1000–5000. The porosity was estimated using a weighting method based on eq. (1)[14]:

$$p = \frac{m_w - m_0}{m_a - m_0} \times 100\% \quad (1)$$

where p is the porosity (%), and m_w, m_0, and m_a are the weight of fiber in water, air, and original, respectively.

The adsorption was studied by recording the UV spectra of ACFs and using the methylene blue solution, for example, 10 mL/g, as absorbent.[14,18]

RESULTS AND DISCUSSION

LPF resin characterization

The FTIR spectra of lignin–phenol–formaldehyde (LPF) resin, neat resin, and original lignin were presented and compared in Figure 1. Observe the most characteristic infrared bands of lignin located at about 1500 and 1600 cm^{-1} representing the C=C aromatic skeletal vibrations. At 3400 cm^{-1}, the stretching vibration appears due to the presence of —OH. The peaks located at 1260 and 876 cm^{-1} are two typical adsorption peaks contributed by the guaiacyl groups of lignin. The 1100 cm^{-1} is the C—H vibration of the syringyl group in lignin. In this synthesis process, the formaldehyde caused an electrophilic addition reaction toward the active positions of benzene rings, and the addition reaction occurred between the formaldehyde and C_5 position of benzene ring in the guaiacyl group of lignin. Because both the C_3 and C_5 positions in relation to the syringyl groups they connected with the methoxy groups, respectively, while hard to react with formaldehyde, this leads the guaiacyl groups of lignin of importance to react with formaldehyde as Figure 2 described.

A comparison of four LPF resins with different lignin contents found that these samples have the same characteristic peaks suggesting the formation of same chemical structure. This means that the variety of lignin content does not affect the chemical structure of LPF resins. However, it should be addressed, because the increasing of lignin content has been found to cause the increase in intensities for some peaks located between 3420 and 3430 cm^{-1} and the decrease in intensities for peaks located at 2920 and 1470 cm^{-1} representing the vibration of C—H in CH_3 and CH_2, respectively. Additionally, the similar decrease in intensity was also found for the peak located at 876 cm^{-1} representing the guaiacyl groups of lignin. The decrease of the C—H intensity suggested that the formaldehyde caused electrophilic addition that lead the active H reacted on the guaiacyl groups of lignin. In other words, this means that the activity of —OH would be strongly to benefit the —OH groups to react with other groups.

The main intense peaks presented in Figure 1 were assigned according to literature[19,20] and summarized in Table I.

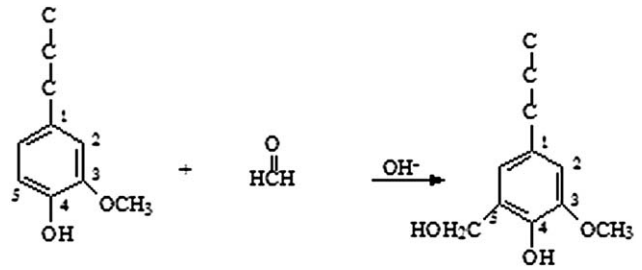

Figure 2 Addition reaction occurred between formaldehyde and the C_5 position of benzene ring in guaiacyl groups of lignin.

TABLE I
IR Peaks Assignments for Lignin and LPF Resin

Wavenumber (cm^{-1})	Assignments[a]
876	γ(C—H); C_2, C_5, C_6 in guaiacyl group
1020–1030	s(C—O); aliphatic —OH and —O—
1100	s(C—H); syringyl group
1210–1220	s(C—O); phenolic hydroxyl and ether group
1260	s(C—O); guaiacyl group
1430	s(C—C); aromatic ring skeleton
1470–1480	δ_a(CH,CH2)
1516	γ(aromatic skeleton)
1620	s(C=C); aromatic
2920	s(C—H); saturated
3420	s(phenolic and aliphatic —OH)

[a] γ: out-of plane twisting or wagging; s: stretching vibration; δa: asymmetric bending; υ: bending mode.

The weight losses of these prepared LPF resins traced by TG were described by recorded TG/DTG curves and showed in Figure 3, where each sample corresponding to one lignin content varied from 0, 8, 14 to 20%, respectively.

As known if there is only a single degradation process, the simple methods have been implemented to treat the thermal degradation of materials. However, when the decomposition occurs through different processes, the analysis is not so simple, especially when these processes may appear in overlapping temperature ranges.[21] According to characteristics values of these TG/DTG curves (Fig. 3) and reference,[22] the degradation processes for these resins have three stages. In the first stage, which related to temperature below 300°C, a relatively low percentage of the weight was lost mainly due to the release of excess phenol, aldehyde, absorbed water, and the water of by-product due to the continue synthesis of resin from resol to resitol and to resite. The second stage was occurred within the range of 300–650°C that results in the formation of some products such as the CO, CO_2, benzaldehyde, phenol, and its polymers with random chain scission and the initial formation of char, and, in this temperature range, most of the polymers decomposition took place. In the third stage, when the temperatures above 650°C, the dehydration greatly occurred, and a carbon-link structure (char) was thus gradually formed, generating carbon monoxide as by-products.

Characteristic values obtained from the TG and DTG curves of four different lignin content samples (Fig. 3) are summarized in Table II, where the TD_M is the temperature at which the maximum rate of degradation occurs, and obtained from the peak of DTG, namely as $(dTG/dt)_M$. The M_f is the final weight rate of the sample. T_{ONSET} is defined as the temperature at which the decomposition initiates. According to Table II and to compare with the neat resin, the temperature ranges of step II of resins, which contained lignin content become small, the

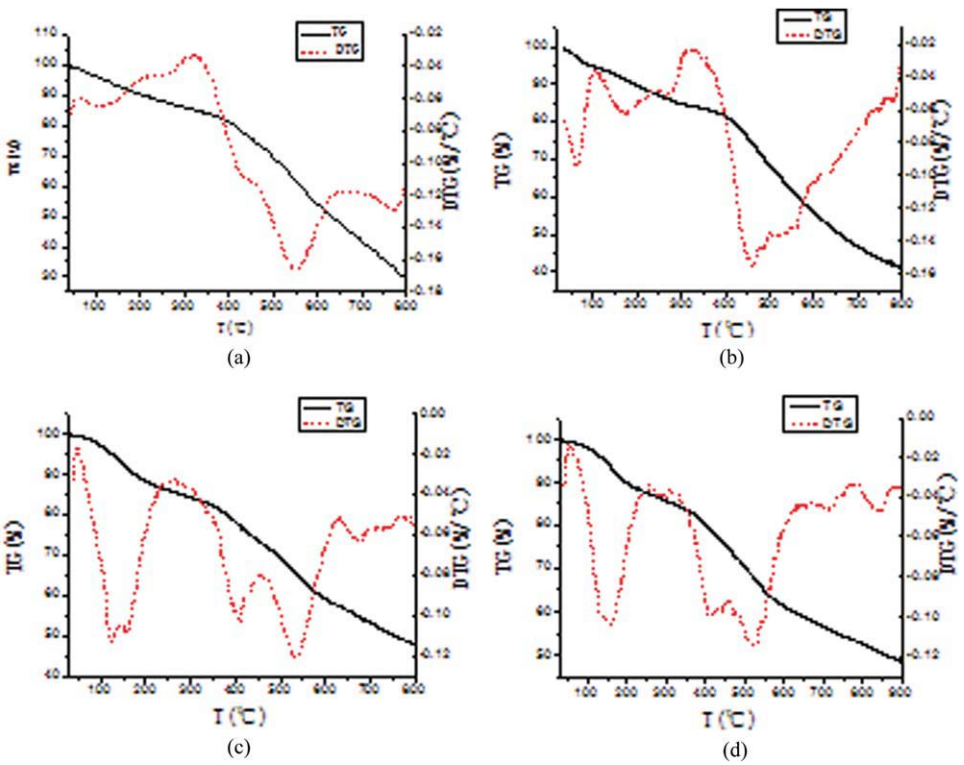

Figure 3 TG/DTG curves of ACFs with different lignin contents. [Color figure can be viewed in the online issue, which is available at wileyonlinelibrary.com.]

TABLE II
Thermal Degradation Values of the LPF Resins During Thermal Treatments

Sample	Curve	Step I	Step II	Step III	M_f (%) $_{800°C}$
1. Neat resin	Temp. range (°C)	53–257	257–643	643–800	29.45
	Weight loss (%)	12.61	39.92	19.02	
	TD_M (°C)	111	553	–	
2. Lignin content 8% resin	Temp. range (°C)	38–266	266–555	555–800	41.02
	Weight loss (%)	13.76	28.61	19.98	
	TD_M (°C)	63, 172	461	–	
3. Lignin content 14% resin	Temp. range (°C)	44–264	264–631	631–800	47.56
	Weight loss (%)	14.53	28.37	9.74	
	TD_M (°C)	120, 159	406, 534	–	
4. Lignin content 20% resin	Temp. range (°C)	53–260	260–641	641–800	52.63
	Weight loss (%)	13.03	27.53	6.54	
	TD_M (°C)	153	405, 524	–	

T_{ONSET}s are shifting to a higher temperature, although the change is tiny only 5–8°C. A further comparison of these samples found that the one with higher content of lignin has a higher temperature range in step II and a higher final weight lose rate. This thermobehavior is considerable, because lignin is a complex, heterogeneous, and three-dimensional polymer, which was formed from the enzyme-initiated dehydrogenative free-radical polymerization of cinnamyl alcohol-based precursors,[14] and this leads some small molecules such as phenol and aldehyde to come into the interior of lignin. Besides, lignin has the aldehyde and phenolic hydroxyl groups; this benefits to react with the phenol/aldehyde effectively.[14] During the carbonization process, two kinds of carbon structures were formed, one is the "hard carbon" formed from phenol and formaldehyde, and another is the "soft carbon" formed from lignin.[14] Because of the three-dimensional structure of lignin, the hollow "soft carbon" is reasonably filled with "hard carbon" to prevent the latter easily degradation. A relative scheme was described in Figure 4.

The results of EA on the ASFs, preoxidized fibers, POFs, and ACFs with 20% lignin content were summarized in Table III. A comparison of these values found that the ACFs have a higher carbon content than that of ASFs indicating the ACFs structured by carbon. The degree of preoxidation is found to cause a higher oxygen percentage to imply the process of this thermal stage that leads the formation of more stable ring structures between the benzene rings by the C—O groups. These structures may benefit the fiber maintaining its form to reduce the influence from the melting deformation in the next thermal stage. ACFs have been also found with slightly higher nitrogen content, and this was perhaps caused by carbonization related nitrogen atmosphere due to little nitrogen reacted with LPF resin to increase the nitrogen content.

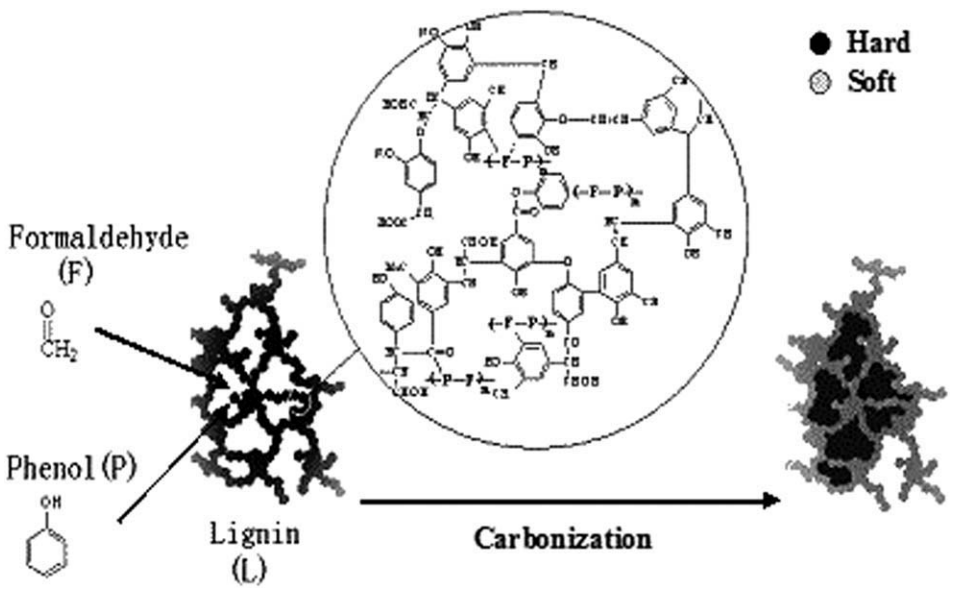

Figure 4 Schematic representation of the PFL resin structure.

TABLE III
Elemental Analyses of As-Spun Fibers, Preoxidized Fibers, and Activated Carbon Fibers, with 20% Lignin Content

Samples	C (%)	H (%)	N (%)	O (%)
ASFs	67.25	5.774	<0.100	26.876
POFs	59.96	3.008	<0.100	36.932
ACFs	91.88	0.822	0.290	7.008

ACFs characterization

The SEM photographs of CF samples with lignin contents varied from 8, 14 to 20% are showed in Figure 5, respectively.

A comparison of the SEM photographs on these ACFs with lignin content at 8 and 14% found that their pores presented in a very wide range, for example, the bigger ranged from 5 to 15 μm and the smaller ranged from 0.5 to 1.5 μm. Noted Figure 5(e–f) showed an obviously different phenomenal for ACFs with lignin content at 20% when compared with other two ACFs [Fig. 5(a–d)], because all pores of the 20% lignin content-based ACFs are observed in the range of 100–800 nm and the pore size distribution in narrow. To compare this work obtained ACFs with literature reported, ACFs[7,11,23] found that there are two differences between these ACFs, the first is that the traditional ACFs were prepared by steam activation, and before steam activation, the fibers have been carbonized. The chemical activity of the surface of the fibers was thus very low, and the chemical etching was hard to carry out by steam and CO_2. Additionally, because the graphite-like structure was formed in ACFs, the pores were hard

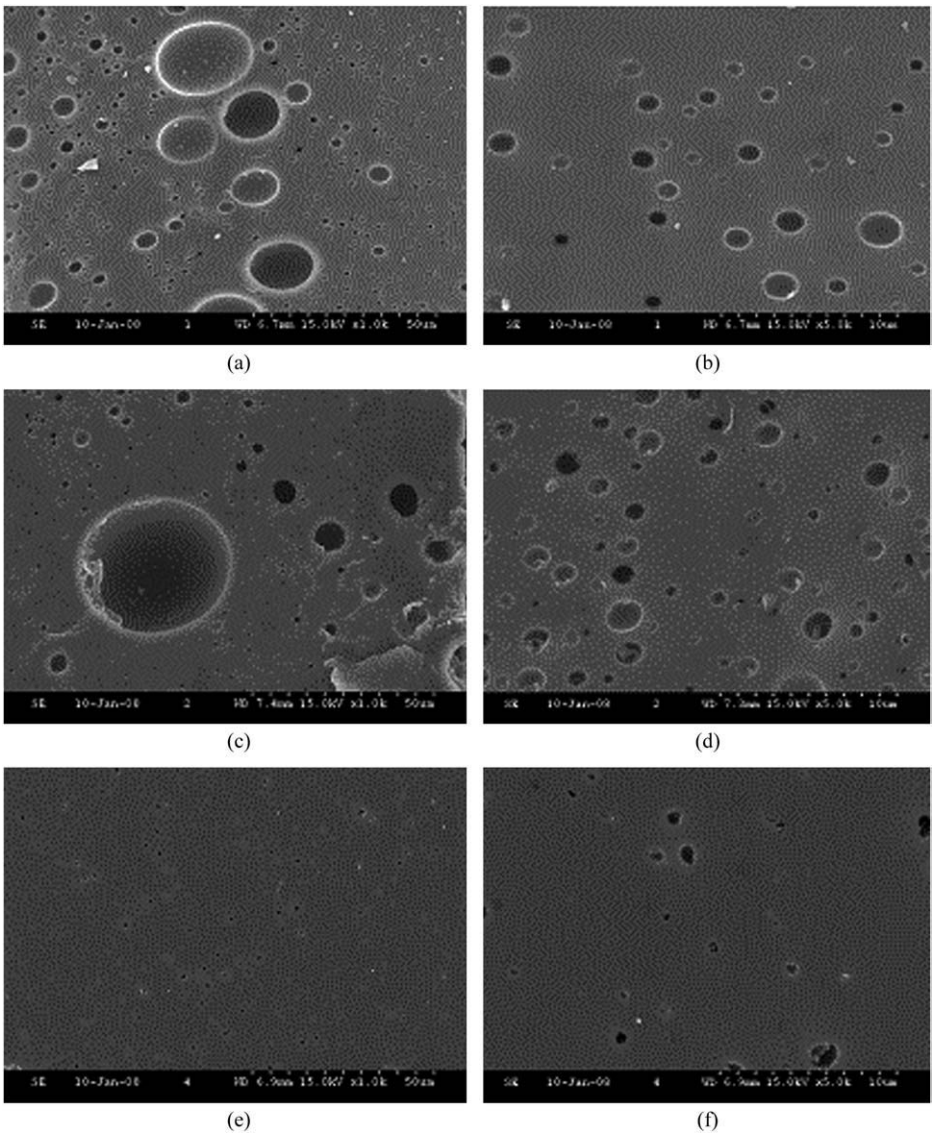

Figure 5 SEM photographs of ACFs with 8% lignin content (a) enlarged by 1000 times, (b) enlarged by 5000 times, with 14% lignin content, (c) enlarged by 1000 times, (d) enlarged by 5000 times, with 20% lignin content, (e) enlarged by 1000 times, and (f) enlarged by 5000 times.

TABLE IV
Porosity and Adsorption Properties of ACFs with Different Lignin Contents

ACFs	Lignin (%)	Porosity (%)	UV adsorption (a.u)
1	8	21.7	0.58
2	14	22.4	0.64
3	20	19.9	0.23

to extend. This means that the traditional methods were hard to get macrospore ACFs. Although in this work, there was not an individual step of activation, because the whole activation process went along with the carbonization process. Therefore, small molecules such as the steam water and formaldehyde would be released during the preoxidation stage. At that time, the precursor fibers have been not formed the graphite-like structure, so that the gas can distract the macromolecular chain segment to form macrospores. The second difference is, in this work, the lignin was directly used as a raw material and its three-dimensional structure would restrict the oversize pore formation and to play a role as pore size controller.

The adsorption data of ACFs were presented in Table IV where the comparison of these data indicates that the 14% lignin content-resulted ACFs have the max porosity and UV adsorption. This suggests that the ACFs could be fabricated under optimized condition, and the lignin content is of importance parameter.

CONCLUSIONS

Experiment has proven that the utilization of lignin as a precursor can cause resulted activated carbon fibers, ACFs, with controllable pore size. The three-dimensional structure of lignin effectively prevents the phenolic resin from easily degradation and meanwhile prevents the oversize pore forming. The lignin content is of importance for controlling the pore structure of ACFs.

References

1. Alcañiz-Monge, J.; De La Casa-Lillo, M. A. Cazorla-Amorós, D.; Linares-Solano, A. Carbon 1997, 35, 291.
2. Mays, T. J. Carbon Materials for Advanced Technologies; New York: Pergamon, 1999.
3. Wigmans, T. Carbon 1989, 27, 13.
4. Shioya, M.; Ojima, T.; Yamashita, J. Carbon 2001, 39, 1869.
5. Zárate, C. N.; Aranguren, M. I.; Reboredo, M. M. J Appl Polym Sci 2008, 107, 2977.
6. Raymundo-Piñero, E.; Cazorla-Amorós, D. Linares-Solano, A.; Find, J.; Wild, U.; Schlögl, R. Carbon 2000, 40, 597.
7. Mamura, R.; Matsui, K.; Ozaki, J.; Oya, A. Carbon 1998, 36, 1243.
8. Lenghous, K.; Qiao, G. G.; Solomon, D. H.; Gomez, C.; Rodriguez-Reinoso, F.; Sepulveda-Escribano, A. Carbon 2002, 40, 743.
9. Tennison, S. R. Appl Catal A 1998, 173, 289.
10. Mangun, C. L.; Daley, M. A.; Braatz, R. D.; Economy, J. Carbon 1998;36:123.
11. Nakagaw, K.; Mukai, S. R.; Tamura, K.; Tamon, H. Chem Eng Res Des 2007, 85, 1331.
12. Fengel, D.; Wegener, G. In Wood: Chemistry, Ultrastructure, Reactions; W. de Gruyter: Berlin, 1984.
13. Hon, D. N. S., Ed. Chemical Modification of Lignocellulosic Materials; Dekker: New York, 1996.
14. Shen, Q.; Zhong, L. Mater Sci Eng A 2007, 445, 731.
15. Teng, H.; Chang, Y. J.; Hsieh, C. T. Carbon 2001, 39, 1981.
16. Jenkins, G. M.; Kawamura, K. Polymeric Carbon: Carbon Fiber Glass and Char; Cambridge University Press: New York, 1976.
17. Oya, A.; Yoshida, S.; Alcaniz-Monge, J.; Linares-Solano, A. Carbon 1995, 33, 1085.
18. Lafyatis, D. S.; Tung, J. H.; Foley, C. Ind Eng Chem Res 1991, 30, 865.
19. Dawy, M.; Shabaka, A. A. A.; Nada, M. A. Polym Degrad Stab 1998, 62, 455.
20. Tejado, A.; Peña, C.; Labidi, J.; Echeverria, J. M. Bioresour Technol 2007, 98, 1655.
21. Yang, J.; Kaliaguine, S.; Roy, C. Rubber Chem Technol 1993, 66, 213.
22. Knop, A.; Pilato, L. Phenolic Resins; Springer-Verlag: New York, 1985; Chapter 8.
23. Tsai, J. H.; Chiang, H. M.; Huang, G. Y.; Chiang, H. L. Hazard J Mater 2008, 154, 1183.